ELSEVIER

Journal of Hazardous Materials B99 (2003) 71–88

Journal of Hazardous Materials

www.elsevier.com/locate/jhazmat

Numerical analysis for electrokinetic soil processing enhanced by chemical conditioning of the electrode reservoirs

Jin-Soo Park, Soon-Oh Kim[1], Kyoung-Woong Kim, Byung Ro Kim, Seung-Hyeon Moon*

Department of Environmental Science and Engineering, Kwangju Institute of Science and Technology (K-JIST), 1 Oryong-dong, Buk-gu, Gwangju 500-712, South Korea

Received 25 July 2002; received in revised form 24 January 2003; accepted 25 January 2003

Abstract

A numerical analysis was undertaken for enhanced electrokinetic soil processing. To perform chemical conditioning of the electrode reservoirs, the electrokinetic soil process employed a membrane as a barrier between the electrode reservoirs and the contaminated soil. An alkaline solution was purged in the anode reservoir that was bounded by the membrane. A mathematical model was used for demonstration of pH change and phenol removal from a kaolinite soil bed, the prediction of pH variations in both electrode reservoirs, and the determination of an optimized injection time of the anode-purging solution. The time-dependent dispersion coefficient was employed in consideration of the averaging effect of the velocity profile on a one-dimensional transport. The estimation of pH and phenol profiles in the soil bed reasonably agreed with the experimental data. The simulation revealed that the removal efficiency of phenol from the kaolinite soil could be improved by maintaining pH of the anode solution.

Keywords: Numerical analysis; Chemical conditioning; Electrokinetic soil process; Membrane; Phenol

1. Introduction

In situ remediation and treatment of contaminated soil and groundwater in hazardous waste sites pose a significant issue to the environment, and such an issue implies very

* Corresponding author. Tel.: +82-62-970-2435; fax: +82-62-970-2434.
E-mail address: shmoon@kjist.ac.kr (S.-H. Moon).
[1] Present address: Department of Earth and Environmental Sciences, College of Science, Korea University, 1, 5ga, Anam-dong, Sungbuk-gu, Seoul 136-701, South Korea.

0304-3894/03/$ – see front matter © 2003 Elsevier Science B.V. All rights reserved.
doi:10.1016/S0304-3894(03)00038-4

difficult technological challenges. Technologies, such as bioremediation, vapor extraction, and pump-and-treat processes, which are aimed at addressing problems of this kind, have been found ineffective when utilized in soils with low permeability [1–6].

Page and Page have excellently provided a comprehensive review on electrokinetic remediation of soils [7]. Electrokinetic soil processing is a promising technology for cleaning up soils or slurries contaminated with certain radionuclides, heavy metals, or organic compounds [8]. This process applies a low-level direct current (dc) between a pair of electrodes placed in a contaminated soil to establish an electric field. As soil contaminants are transported towards one of the electrodes due to the electric field, they may then be removed from the soil bed. Two main mechanisms are responsible for this transport: electromigration and electroosmosis. In electromigration, positively charged ions move toward the cathode while negatively charged ions move to the anode. Electrolysis of water, which produces hydrogen ions at the anode and hydroxyl ions at the cathode, will lower the pH level around the anode and help metal-precipitates dissolve. The dissolved metal cations then move to the cathode, while hydroxyl ions produced around the cathode move to the anode through electromigration. In electroosmosis, a thin layer of positively charged fluid (i.e. the diffused electrical double layer that contains concentrated cations) adjacent to the negatively charged pore wall is pulled toward the cathode. This results in the overall pore liquid movement toward the cathode.

Another transport mechanism involved in the electrokinetic processes is electrophoresis. Electrophoresis, convection of the bulk liquid, accompanies the movement of charged colloidal particles under an applied electric field. However, colloidal transport is not a dominant mechanism in a compact soil with low permeability [9]. In this case, the convection of the bulk liquid is also negligible.

Hydrogen ions and hydroxyl ions generated at the electrodes can adversely affect the efficiency of the electrokinetic process. In normal electrokinetic soil processing, the production of those ions could lead to a pH level below 2 at the anode and above 10 at the cathode in the soils with a low buffering capacity [10–12]. The mobility of protons is approximately twice as great as that of hydroxyl ions. Therefore, the acid front associated with protons propagates toward the cathode much faster than the base front associated with hydroxyl ions. In the removal of inorganic contaminants, metal hydroxide precipitation occurs near the cathode causing also severe voltage drop between the electrodes in the soil, which then increases power consumption. In removing organic contaminants, the protons, which are propagating from the anode, reduce the zeta potential of the soil surface because the protons were adsorbed at the surface of negatively charged soil particles. The reduction in zeta potential leads to a lower electroosmotic velocity according to the Helmholtz–Smoluchowski relation [13].

$$u_{\mathrm{eo}} = -\frac{\varepsilon \zeta E_x}{\mu} \tag{1}$$

where ϵ is the permittivity of the pore liquid, ζ the zeta potential of the soil, E_x the electric field parallel to the direction of the electroosmotic flow, and μ the viscosity of the pore liquid.

Puppala et al. [14] suggested the following procedures to avoid the aforementioned situation and enhance the transport of contaminants: (1) periodically flush the area near either or both electrodes using a fluid with a controlled pH and chemistry (conditioning fluid), (2)

neutralize pH changes caused by electrolysis reactions by allowing the base/acid front to move across the soil, (3) introduce complexing agents that form complexes with metal contaminants during transport, and (4) use special electrodes or membranes around electrodes to control the chemistry near the electrodes.

The experimental data presented by Kim et al. [13] examined the use of a porous membrane around electrodes for the phenol removal using chemical conditioning of electrode reservoirs. Since electrode reservoirs could be chemically conditioned for pH control in this scheme, the removal of phenol was enhanced by increased electroosmosis. This phenomenon was described using a mathematical model by altering boundary conditions. The objectives of this study were: (1) to develop a mathematical model in describing the behaviors of proton and phenol (C_6H_5OH) in an aqueous phase of a soil bed, and (2) to mathematically evaluate the efficiency of chemical conditioning of electrode reservoirs in the enhanced transport of soil contaminants.

2. Description of the mathematical model

The following assumptions are applied in development of the mathematical model used in this study: (1) the porous medium is saturated and is negatively charged, (2) all fluxes are linear functions of potential and hydraulic gradients, (3) the temperature is uniform, (4) the chemical reactions are at instantaneous equilibrium, and (5) the soil is treated as an electrically non-conductive material. The total flux of contaminant species i can be described for a one-dimensional space based on diffusion (Fick's first law), electromigration (Nernst–Townsend–Einstein relation), electroosmosis (Helmholtz–Smoluchowski relation), and hydraulic flow (Darcy's law) [15,16].

$$J_i = -D_i^* \frac{\partial c_i}{\partial x} - c_i (u_i^* + k_e) \frac{\partial E}{\partial x} - c_i k_h \frac{\partial h}{\partial x}; \quad i = 1, 2, \ldots, N \tag{2}$$

associated with the following relations:

$$D_i^* = D_i \tau n \tag{3}$$

$$u_i^* = u_i \tau n = \frac{D_i^* z_i F}{RT} \tag{4}$$

$$k_e = \frac{\varepsilon \zeta}{\tau^2 \mu} \tag{5}$$

where J_i is the total mass flux of the chemical species i per unit cross-sectional area of the porous medium, D_i^* the effective diffusion coefficient of the chemical species i, c_i the molar concentration of the chemical species i, u_i^* the effective ionic mobility of the chemical species i, k_e the coefficient of electroosmotic permeability, E the electric potential, k_h the hydraulic conductivity, h the hydraulic head, D_i the diffusion coefficient of the chemical species i, τ the empirical tortuosity, n the porosity, u_i the ionic mobility of the chemical species i, z_i the charge of the chemical species i, F the Faraday's constant, 96485 C/mol, R the universal gas constant, 8.314 J/(K/mol), T the absolute temperature, and N the number of chemical species.

The conservation of mass in a control volume of the porous medium, which contains both liquid and solid phases, leads to:

$$\frac{\partial nc_i}{\partial t} = -\frac{\partial J_i}{\partial x} \pm nR_i \tag{6}$$

where R_i represents the net volumetric rates of production of species i due to sorption.

Incorporating Eq. (2) into Eq. (6),

$$\frac{\partial nc_i}{\partial t} = D_i^* \frac{\partial^2 c_i}{\partial x^2} + \left[(u_i^* + k_e) \frac{\partial E}{\partial x} + k_h \frac{\partial h}{\partial x} \right] \frac{\partial c_i}{\partial x} \pm nR_i \tag{7}$$

R_i can be described if the sorption of soil contaminants is assumed to be linear.

$$R_i = -\frac{\rho}{n} \frac{\partial q_i}{\partial t} = -\frac{\rho}{n} \frac{\partial q_i}{\partial c_i} \frac{\partial c_i}{\partial t} = \frac{\rho}{n} K_i^p \frac{\partial c_i}{\partial t} \tag{8}$$

where ρ is the dry bulk density and q_i the mass of adsorbed species i per unit mass.Combining Eqs. (7) and (8),

$$R_i^d \frac{\partial nc_i}{\partial t} = D_i^* \frac{\partial^2 c_i}{\partial x^2} + \left[(u_i^* + k_e) \frac{\partial E}{\partial x} + k_h \frac{\partial h}{\partial x} \right] \frac{\partial c_i}{\partial x} \tag{9}$$

where the retardation factor for species i, R_i^d is described as:

$$\left(1 + \frac{\rho}{n} K_i^p\right) = R_i^d \tag{10}$$

where K_i^p the solid/liquid phase partition coefficient for the chemical species i [16–19]. Rewriting Eq. (9),

$$R_i^d \frac{\partial nc_i}{\partial t} = D_i^* \frac{\partial^2 c_i}{\partial x^2} + [u_{eo} + u_{ei} + u_h] \frac{\partial c_i}{\partial x} \tag{11}$$

associated with the following relations:

$$u_{ei} = u_i^* \frac{\partial E}{\partial x} \tag{12}$$

$$u_{eo} = k_e \frac{\partial E}{\partial x} \tag{13}$$

$$u_h = k_h \frac{\partial h}{\partial x} \tag{14}$$

where, u_{ei} is the electromigration velocity, u_{eo} the electroosmotic velocity, and u_h the interstitial velocity.

The electroneutrality condition is as follows:

$$\sum_{j=1}^{N} z_j c_j = 0 \tag{15}$$

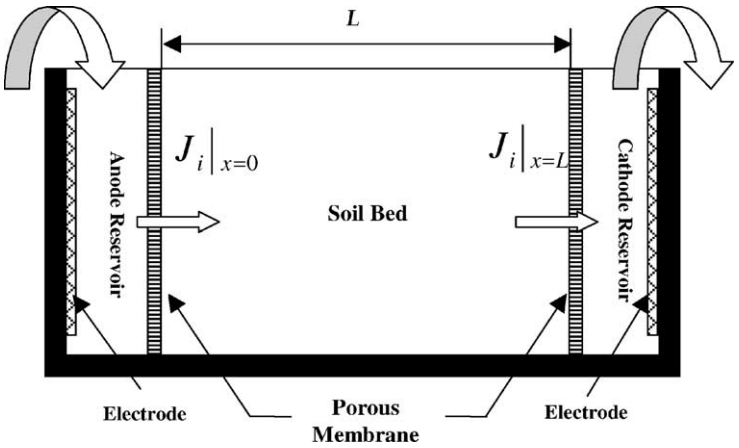

Fig. 1. A schematic diagram of experimental equipment.

Boundary conditions for the total hydraulic head at the electrode reservoirs are zero.

$$h|_{x=0} = h|_{x=L} = 0 \tag{16}$$

where L is the total distance of a soil bed (see Fig. 1).

Boundary conditions for the total flux of species i are:

$$J_i = -D_i^* \frac{\partial c_i}{\partial x} - (u_{ei} + u_{eo})c_i; \quad x = 0 \tag{17}$$

$$J_i = -D_i^* \frac{\partial c_i}{\partial x} - (u_{ei} + u_{eo})c_i; \quad x = L \tag{18}$$

For determination of the boundary conditions for the fluxes of proton and hydroxyl ion, each concentration of them in the both reservoirs should be considered. Two main water electrolysis reactions occur at each electrode. At an anode the reaction is as follows:

$$2H_2O \rightarrow 4H^+(aq) + O_2(g) + 4e^-. \tag{19}$$

While at cathode:

$$2H_2O + 2e^- \rightarrow 2OH^-(aq) + H_2(g). \tag{20}$$

The pH of an anode-purging solution decreases due to the generation of protons, whereas the pH of a cathode-purging solution increases due to the generation of hydroxyl ion. The respective fluxes for the generation of proton at an anode and hydroxyl ion at a cathode are:

$$J_{H^+} = \frac{\eta_{H^+} I_{H^+}}{F} \tag{21}$$

and

$$J_{OH^-} = \frac{\eta_{OH^-} I_{OH^-}}{F} \tag{21}$$

where η_i is the efficiency of electrode for the chemical species i and I the current applied along the soil. The efficiency of an electrode in generating protons at the anode and hydroxyl ions at the cathode is assumed to be in unity, that is, all electric current is consumed for the electrode reactions.

If neither acid nor base is added to the electrode reservoirs, the concentration of protons at the anode and cathode reservoirs, respectively, are given as follows:

$$c_{H^+} = 2K_w \left[-\frac{IA\,\Delta t}{FV_{reservoir}} + \left(\left(\frac{IA\,\Delta t}{FV_{reservoir}} \right)^2 + 4K_w \right)^{1/2} \right]^{-1} \tag{22}$$

$$c_{H^+} = \frac{1}{2} \left[-\frac{IA\,\Delta t}{FV_{reservoir}} + \left(\left(\frac{IA\,\Delta t}{FV_{reservoir}} \right)^2 + 4K_w \right)^{1/2} \right] \tag{23}$$

where K_w is the equilibrium constant for auto-ionization reaction of water (10^{-14} mol^2/l^2), A the cross-sectional area of the system, Δt the time step between a new point and an old point, and $V_{reservoir}$ the volume of each reservoir.

If x M (mol/l) of a base is added to the anode reservoir, the concentration of the proton will be:

$$c_{H^+} = \frac{1}{2} \left[-\left(xn - \frac{IA\,\Delta t}{FV_{reservoir}} \right) + \left(\left(xn - \frac{IA\,\Delta t}{FV_{reservoir}} \right)^2 + 4K_w \right)^{1/2} \right] \tag{24}$$

where n is the number of electron associated with the chemical reaction.

If y M of an acid is added to the cathode reservoir, the concentration of the proton will be:

$$c_{H^+} = 2K_w \left[-\left(yn - \frac{IA\,\Delta t}{FV_{reservoir}} \right) + \left(\left(yn - \frac{IA\,\Delta t}{FV_{reservoir}} \right)^2 + 4K_w \right)^{1/2} \right]^{-1} \tag{25}$$

The aforementioned governing equations along with the boundary conditions were solved numerically using an explicit *forward time and centered space* (FTCS) scheme. Time derivatives were discretized using the finite forward difference method, and spatial derivatives were discretized by the finite central difference method to convert the governing partial differential equations to a system of algebraic equations. The spatial derivative was evaluated at the nth time level, i.e. at a known time level with a linear variation in electrical potential and in hydraulic potential head across the soil bed [20].

The model used in this study has involved all the charged species such as H^+, OH^-, Na^+, and SO_4^{2-}, and a non-charged species, phenol (as far as the solution pH is below its pK_a value, 9.9) existing in the aqueous phase of the soil bed by using three of the four transport equations for the major charged species such as H^+, OH^-, Na^+, and SO_4^{2-}, and one for

Table 1
Parameters used in numerical analysis

Parameter	Value	Reference
Length of soil bed (cm), L	15	[13]
Applied voltage (V), E	15	[13]
Porosity, n	0.52	[13]
Tortuosity, τ	1.25	[26]
Hydraulic permeability (m^2/(Pa s)), k_h	10^{-10}	[26]
Permittivity of the pore liquid (F/m), ϵ	7.0×10^{-10}	[26]
Viscosity of the pore liquid (Pa s), μ	10^{-3}	[26]
Phenol concentration (mol/l)	5.32×10^{-3}	[13]
Diffusion coefficient of H^+ (m^2/s), D_{H^+}	9.31×10^{-9}	[25]
Diffusion coefficient of OH^- (m^2/s), D_{OH^-}	5.27×10^{-9}	[25]
Diffusion coefficient of Na^+ (m^2/s), D_{Na^+}	1.33×10^{-9}	[25]
Diffusion coefficient of $SO_4{}^{2-}$ (m^2/s), $D_{SO_4{}^{2-}}$	1.06×10^{-9}	[25]
Diffusion coefficient of C_6H_5OH (m^2/s), $D_{C_6H_5OH}$	1.00×10^{-9}	[26]
Diffusion coefficient of $C_6H_5O^-$ (m^2/s), $D_{C_6H_5O^-}$	1.09×10^{-9}	[26]
Mobility of H^+ (m^2/(V/s)), u_{H^+}	3.62×10^{-7}	[27]
Mobility of OH^- (m^2/(V/s)), u_{OH^-}	2.06×10^{-7}	[27]
Mobility of Na^+ (m^2/(V/s)), u_{Na^+}	5.19×10^{-8}	[27]
Mobility of $SO_4{}^{2-}$ (m^2/(V/s)), $u_{SO_4{}^{2-}}$	8.27×10^{-8}	[27]
Mobility of C_6H_5OH (m^2/(V/s)), $u_{C_6H_5OH}$	3.89×10^{-8}	[27]
Mobility of $C_6H_5O^-$ (m^2/(V/s)), $u_{C_6H_5O^-}$	4.23×10^{-8}	[27]

phenol, and an electroneutrality equation to maintain charge balance. Using the electroneutrality equation, one of the transport equations was replaced by an algebraic equation. It was noted the pH variations in the both reservoirs could not be directly used as the flux boundary conditions because the interior of the electrode reservoirs was not included in the control volume of the governing equations (see Fig. 1). However, the concentrations of proton and hydroxyl ion in the both reservoirs were well imposed as those of the numerical domain at the both boundaries since the soil has a low buffering capacity. Therefore, the concentrations of proton and hydroxyl ion in the both reservoirs were calculated by the Eqs. (22)–(25) to determine flux boundary conditions. From the boundary condition at $x = 0$ and a known time, the propagations of each flux were solved from the aforementioned five algebraic equations including the electroneutrality condition along with soil parameters and proportionality constants. Parameters in this numerical analysis are listed in Table 1. The experimental study for the electrokinetic remediation of the soil bed contaminanted by phenol was conducted at a constant current test as shown in Table 2. In order to describe transport of each species in the soil bed using the governing equation, Eq. (11), however, a potential gradient was needed to calculate electromigration and electroosmotic velocity. We observed that the potential variation maintained to be approximately 15 V during the constant current operation, and assumed the constant current test to be the semi-constant voltage test for simplification of the model calculation. Although the local voltage gradient should be calculated from local conductance of the chemical species in an aqueous phase and soil surface within the soil bed by assuming continuity of electrical current for an accurate demonstration by the model [21], it was very difficult to determine the surface conductivity of soil particles.

Table 2
Experimental conditions for the two tests carried out in a previous study for the removal of phenol from the kaolinite soil bed [9]

Conditions	Experiment I	Experiment II
Soil specimen	Kaolinite	Kaolinite
Contaminants	Phenol (C_6H_5OH)	Phenol (C_6H_5OH)
Initial concentration of contaminants (μg/g)	178.2	333.8
Applied current (A)	0.1	0.1
Area of soil cell (cm^2)	81	81
Duration (h)	96	96
Anode-purging solution	0.1 M NaCl solution 2 l	0.1 M NaOH solution 2 l
Cathode electrolyte solution	0.25 M H_2SO_4	0.25 M H_2SO_4

Yeung and Dalta [22] has presented a robust numerical model of electrokinetic transport in which the coupled flows of ionic contaminants were formulated by the formalism of non-equilibrium thermodynamics to describe the simultaneous flows of fluid, electricity, cation, and anion under the combined influences of hydraulic, electrical, and chemical gradients and the resulting change of pH in the pore fluid as a function of time and space by maintaining electrical neutrality. Using the developed numerical model, they showed good agreement between computed and experimental results in a pH gradient, and predicted other main inorganic ions which were involved in electrokinetic transport during treatment of contaminated soils. In this study, we intended to develop a numerical model to predict the phenol removal when enhancing the electrokinetic treatment process using chemical conditioning of the electrode reserviors. We used the porous membrane as a barrier to fix the boundaries of the reservoirs. Each concentration of the chemical species in the reservoirs bounded by the porous membrane was significantly used as boundary conditions to predict the variations of all the species involved in the transport under the electric field such as H^+, OH^-, Na^+, $SO_4{}^{2-}$ and phenol. Especially, concentrations of the proton and hydroxyl ion could be accurately estimated by the electrolytic decomposition of water at the electrode, based on Faraday's law. For chemical conditioning of the electrode reservoir, a base was added into the anode reservoir. Assuming that the instantaneous equilibrium occurred in the reservoir, pH was computed precisely by the suggested equations (Eqs. (22)–(25)), and was used as boundary conditions of the proton and hydroxyl ion. Thereafter, pH profiles across the soil bed by the transport of an acid front during the process were predicted well by the introduction of a time-dependent dispersion coefficient (to be discussed in this study) even though the numerical approach using the coupled flows of ionic contaminants was not considered. Moreover, the continuous pH change during electrokinetic soil processing caused variation of the zeta potential of the soil bed, finally resulting in the change of electroosmotic velocity and/or its direction. The electroosmotic velocity that significantly determines the removal efficiency of phenol in the soil bed is very sensitive to pH of the solution in the pore water. In order to include the phenomena in the model, we used a pH-dependent zeta potential equation of kaolinite beds as determined from streaming potential measurement by Lorenz [23] to determine zeta potentials of the kaolinite bed with respect to pH. The equation is following:

$$\zeta(mV) = -38.6 + 281\,e^{-0.48\,pH}. \tag{26}$$

As a result, phenol profiles were fitted well with the experimental data. It was thought that the estimation of pHs in the reservoir and the time-dependent dispersion coefficient enabled to make accurate prediction of the pH profiles and the phenol profiles in the system.

The schematic of the experimental set-up used by Kim et al. [13] is shown in Fig. 1. Two experiments for removal of phenol were conducted to illustrate application of the model in the enhanced electrokinetic soil processing. Experimental conditions used in the study are summarized in Table 2. Experiments I and II were designed to determine which anode-purging solution was more suitable in removing phenol from the kaolinite soil. Two kilogram of air-dried kaolinite soils were mixed with a liter of 500 mg/l (Experiment I) and a liter of 1000 mg/l (Experiment II) phenol solutions to obtain 50% (w/w) water content. The slurry of soil samples was mechanically mixed for 1 h and was allowed to settle for 2 days to attain a uniform distribution of phenol. Other detailed procedures are described elsewhere [13].

3. Results and discussion

3.1. pH variation in anode and cathode reservoirs

Understanding pH variations in the anode and cathode reservoirs is important for the following reasons: (1) to determine when an acid or base needs to be added in each reservoir, (2) to neutralize proton or hydroxyl ion generated from electrolysis, and (3) to accurately set-up the boundary conditions for the numerical analysis.

The pH variation in both reservoirs is expressed as shown in Eqs. (22) and (25) for Experiment I, and Eqs. (24) and (25) for Experiment II. Fig. 2 shows pH variations with and without chemical conditioning in the reservoirs bounded by the membrane (see Fig. 1). The extreme pH conditions as shown in Fig. 2a are due to generation of proton and hydroxyl ion at each electrode as described in Eqs. (22) and (23). This condition may result in poor removal efficiency due to the decreased electroosmotic velocity by the propagation of the acid front and the reverse migration of phenol, which partly becomes anionic at a pH over 9.9 (pK_a).

Fig. 2b shows the predicted and measured pH variations of both reservoirs when 0.25 M H_2SO_4 cathode-purging solution was added to keep the pH of the cathode reservoir very acidic. Chemical conditioning of the cathode reservoir may prevent the reverse migration of phenol caused by increased pH near the cathode reservoir and then enhance the electrokinetic process. However, the low pH of the anode reservoir could lower the electroosmotic velocity as discussed earlier.

Fig. 2c shows the pH variation of both reservoirs when 0.1 M NaOH anode-purging solution instead of 0.1 M NaCl anode-purging solution was used to neutralize the proton, which was generated at the anode. This will keep the pH of the entire soil bed higher resulting in the increased electroosmotic velocity. In the middle of the operation, the predicted pH of the anode reservoir, however, decreases rapidly after 48 h when no additional base is added in the anode reservoir. As a result, it was necessary to add a fresh anode-purging solution because the hydroxyl ion, which was added initially in the anode reservoir, was completely exhausted due to the quick reaction between H^+ and OH^- to form H_2O. The experimental

data in Fig. 2c also show the pH variations when a fresh anode-purging solution was added to the anode reservoir after 48 h for Experiment II. The pH variation of the anode reservoir predicted by Eq. (24) reasonably agrees with the experimental data with the addition of a fresh solution.

Eqs. (22)–(25) gave the numerical prediction of the pH changes in both reservoirs and the accurate injection time of each additional purging solution in order to maintain the

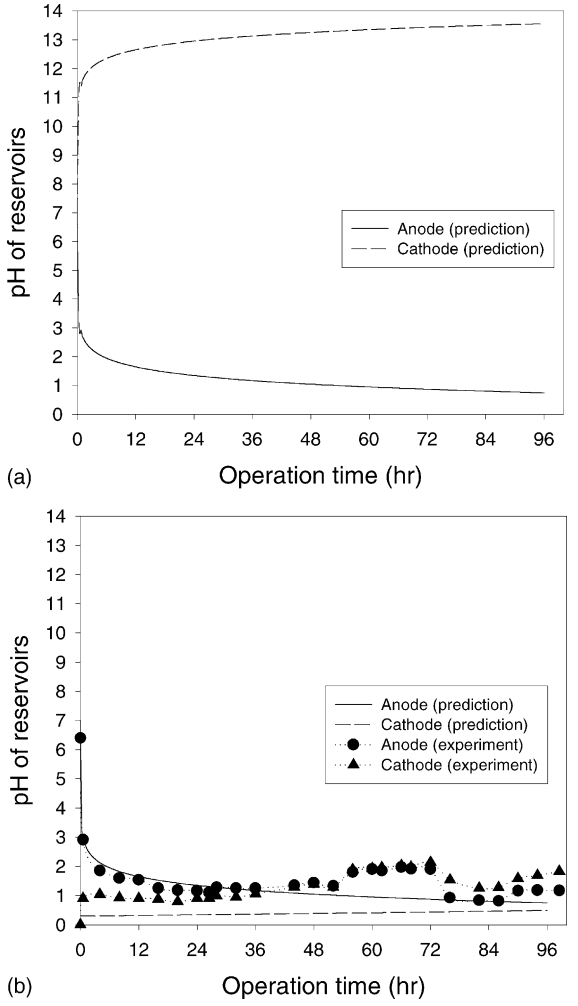

Fig. 2. pH variation in the anode and cathode reservoir: (a) pH variations calculated by Eqs. (22) (solid line) and (23) (dotted line) when no chemical conditioning, (b) comparison of pH variations between the experimental data for Experiment I and calculated data by Eqs. (22) (solid line) and (25) (dotted line) when chemically conditioned in the cathode reservoir with 0.25 M H_2SO_4, (c) comparison of pH variations between the experimental data for Experiment II and calculated data by Eqs. (24) (solid line) and (25) (dotted line) without (solid line) and with addition of 0.1 M NaOH (bold solid line) into the anode reservoir at 48 h.

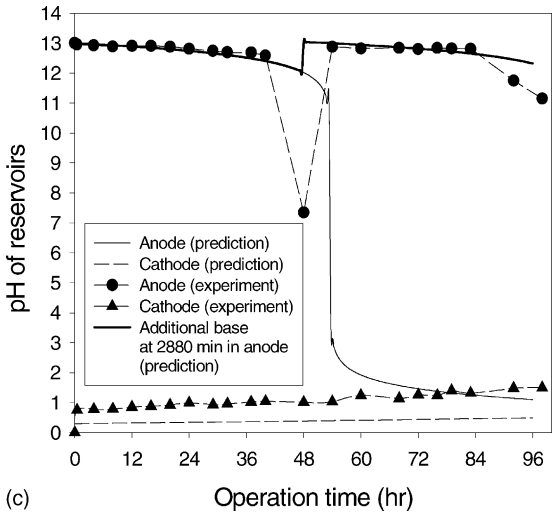

Fig. 2. (*Continued*).

pH of both reservoirs optimal for the electrokinetic process, as discussed earlier. Also, the equations may provide optimum concentrations of anode- and cathode-purging solution from prediction of the pH changes to improve the electrokinetic process and to minimize the use of purging chemical solutions.

3.2. pH profile in the soil bed

Fig. 3a shows pH profiles across the soil bed along with numerical results for Experiment I when chemical conditioning was carried out for the cathode reservoir only. The initial pH of the soil bed was at 6.4. The experimental pH value dropped to about 0.5 within 72 h at the anode region due to the generation of proton. The pH increase in the cathode region was not observed because an acid was added to neutralize the hydroxyl ions generated at the cathode. The pH decreased slightly due to the loss of proton added to the cathode reservoir by the diffusion toward the anode and the propagation of the acid front from the anode. Therefore, the acid front advance from the anode significantly affected the pH profile of the pore water in the soil bed. The predicted pH profiles in Fig. 3a indicate that it is difficult to precisely predict pH change after 1 day. This phenomenon might have been due to underestimation of the effect of the severe heterogeneity of the soil bed. Along with electrokinetic transport, dispersion occurs in the soil bed due to diffusion, mixing, a non-continuous flow path, and the parabolic velocity profile which are caused by heterogeneity of the soil bed. Increment in the diffusion coefficient may improve the agreement with experimental data. Therefore, we employed the time-dependent dispersion coefficient to express the variation of diffusion coefficient as well as to average the parabolic velocity profile of the fluid on a one-dimensional transport. Eq. (11) can be rewritten to include the dispersion effect as shown below.

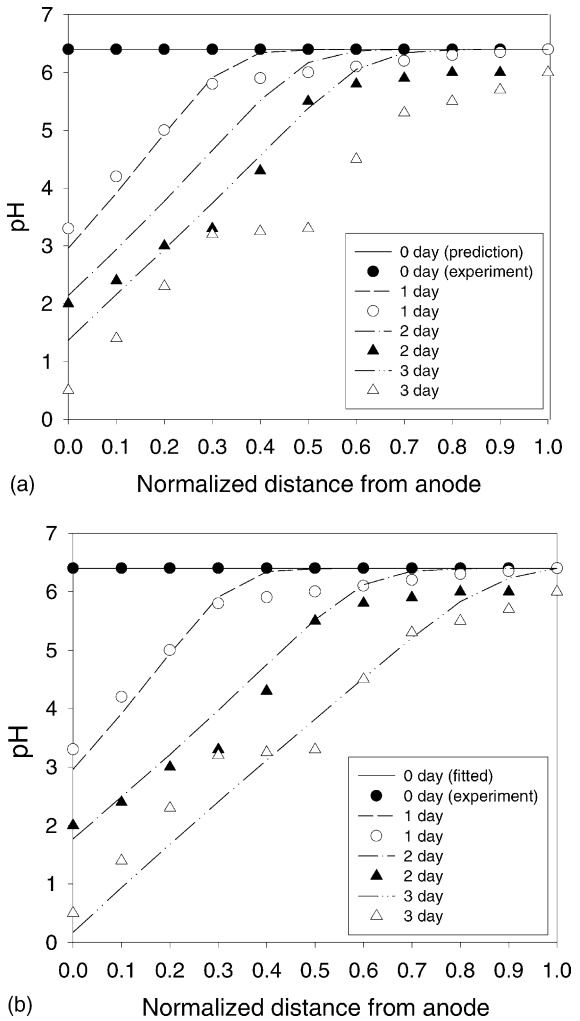

Fig. 3. Numerical analysis of the pH profiles of the pore water in the soil bed for Experiment I with chemical conditioning of 0.25 M H_2SO_4 in the cathode reservoir across the soil bed with the operation time (spots: experimental data and lines: predicted data): (a) comparison between the experimental pH profiles and non-fitted pH profiles in terms of dispersion, (b) comparison between the experimental pH profiles and fitted pH profiles in terms of dispersion.

$$R_i^{\mathrm{d}} \frac{\partial n c_i}{\partial t} = (D_i^* + e_i^*) \frac{\partial^2 c_i}{\partial x^2} + [u_{\mathrm{eo}} + u_{\mathrm{ei}} + u_{\mathrm{h}}] \frac{\partial c_i}{\partial x} \tag{27}$$

or

$$R_i^{\mathrm{d}} \frac{\partial n c_i}{\partial t} = E_i^* \frac{\partial^2 c_i}{\partial x^2} + [u_{\mathrm{eo}} + u_{\mathrm{ei}} + u_{\mathrm{h}}] \frac{\partial c_i}{\partial x} \tag{28}$$

where, e_i^* is the effective dispersion coefficient of the chemical species i and $E_i^*(= D_i^* + e_i^*)$ the overall dispersion coefficient of the chemical species i [24].

To estimate the experimental pH profiles numerically including the average effect of the velocity profile of the fluid in the soil bed, the most suitable time-average mean dispersion coefficient was selected and then the experimental data was fitted. Based on these values, the time-dependence of E_i^* was found to linearly correlated with time. Since the integration of time-dependent dispersion coefficients could eliminate the tendency of the dispersion coefficient to fluctuate with time, applying the time-averaging dispersion coefficient instead of the time-dependent dispersion coefficient is more convenient in line with a well described conservation equation of mass, which is in a control volume of the porous medium containing both the liquid and solid phases. The time-average mean dispersion coefficient can be calculated as follows [24]:

$$\overline{E_i^*} = \frac{1}{t_f - t_i} \int_{t_i}^{t_f} E_i^*(t)\, \mathrm{d}t \tag{29}$$

Finally, Eq. (27) becomes:

$$R_i^{\mathrm{d}} \frac{\partial n c_i}{\partial t} = \overline{E_i^*} \frac{\partial^2 c_i}{\partial x^2} + [u_{\mathrm{eo}} + u_{\mathrm{ei}} + u_{\mathrm{h}}] \frac{\partial c_i}{\partial x} \tag{30}$$

Fig. 3b shows the results of Experiment I with a set of predicted results using the above time-averaging dispersion coefficient. The predicted results agree well with the experimental data. As expected, the pH decreases gradually as the acid front propagates toward the cathode. This is due to the NaCl purging solution of the anode reservoir with no buffering capacity to neutralize the proton produced in the anode.

Electroosmosis is the predominant mechanism in removing organic soil contaminants such as phenol. Because electroosmosis is significantly dependent on soil pH, the soil pH should be controlled to attain the most efficient electroosmosis state as discussed earlier. Therefore, it is necessary to introduce chemical conditioning in the anode reservoir to buffer the proton generated from the associated water electrolysis reaction. In Experiment II where an NaOH purging solution was used to neutralize the hydrogen ion produced in the anode reservoir, a 3D plot of the simulated results is found that the soil pH was only slightly increased near the anode reservoir, and most of the soil bed was kept to be constant at about 6.4, which is the same as the initial pH of the soil bed as shown in Fig. 4. From this pH profile, it can be expected that the electroosmosis may increase in the soil bed, resulting in enhancing the removal of phenol.

3.3. Phenol profile in the soil bed

For Experiment I, the concentration profiles of phenol in the soil bed are shown in Fig. 5a. Both predicted and experimental results show that phenol from the kaolinite soil has been gradually removed up to approximately 75% of its initial concentration in 4 days. The fluctuation in the experimental data for the first 2 days might have been due to the initial non-homogeneity of the soil bed even though the entire bed was initially mixed before the experiment. For Experiment II, where the produced proton was neutralized at the anode (see Fig. 4) by adding the basic purging solution, an increased (84.7%) removal

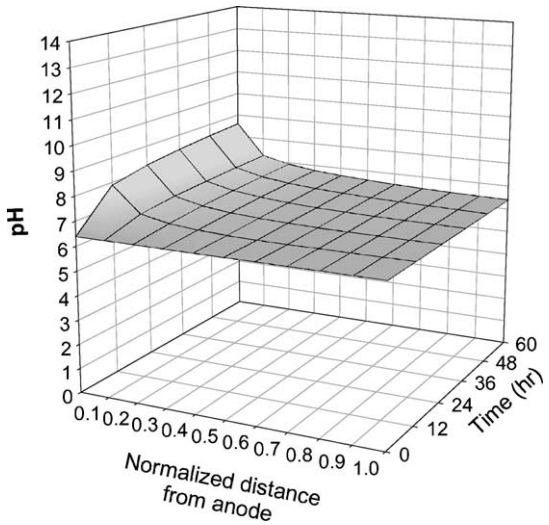

Fig. 4. Numerical prediction of pH profiles of the pore water in the soil bed for Experiment II with chemical conditioning of 0.1 M NaOH and 0.25 M H_2SO_4 in the anode and the cathode reservoir, respectively.

of phenol is observed in 4 days as shown in Fig. 5b. As a result, no chemical conditioning of the anode reservoir (see Figs. 3b) led to reduction in the rate of electroosmotic flow by rapid movements of the acid front, while the chemically conditioned electrokinetic process increased electroosmotic flow as expected. A good agreement between the experimental and predicted data was observed. No accumulation of phenol in front of the membrane of the cathode reservoir was observed, indicating that the membrane used in this study did not interfere with the transport of phenol.

As a result, the selection of a purging solution for the anode and/or the cathode would be the main parameter to enhance the electrokinetic soil process for the removal of phenol. In order to maintain a suitable soil pH for the optimal development of electroosmotic flow, it was necessary to control the basicity of the anode-purging solution. As the pH in the whole soil bed was kept lower than 9.9 in the prediction of the soil pH for Experiment II, phenol existed in neutral form, which was removed by electroosmosis only. If soil pH rose to 9.9 or higher at which phenol turned to an anion, the higher removal of phenol might be attained by electroosmosis as well as electromigration of charged phenol. Fig. 6a shows the predicted pH profile of the soil bed when the purging solution of 4 M NaOH is chemically conditioned at the anode reservoir. However, the pH of the entire soil bed did not increase to 9.9. It was found that the soil pH hardly increased except the soil bed near the anode reservoir because the hydroxyl ion from the anode reservoir moved to an opposite direction against the electric field. Additionally, the fact that the negatively charged soil pores allowed to flow only positively charged fluid constrained the movement of the hydroxyl ion, which was not adsorbed at the surface of soil particles. The predicted result shows that only an additional 2% of phenol (86.1%) was removed from the soil bed compared with that in Experiment II due to a slight increase in the soil pH (see Fig. 6b). Even though the use of

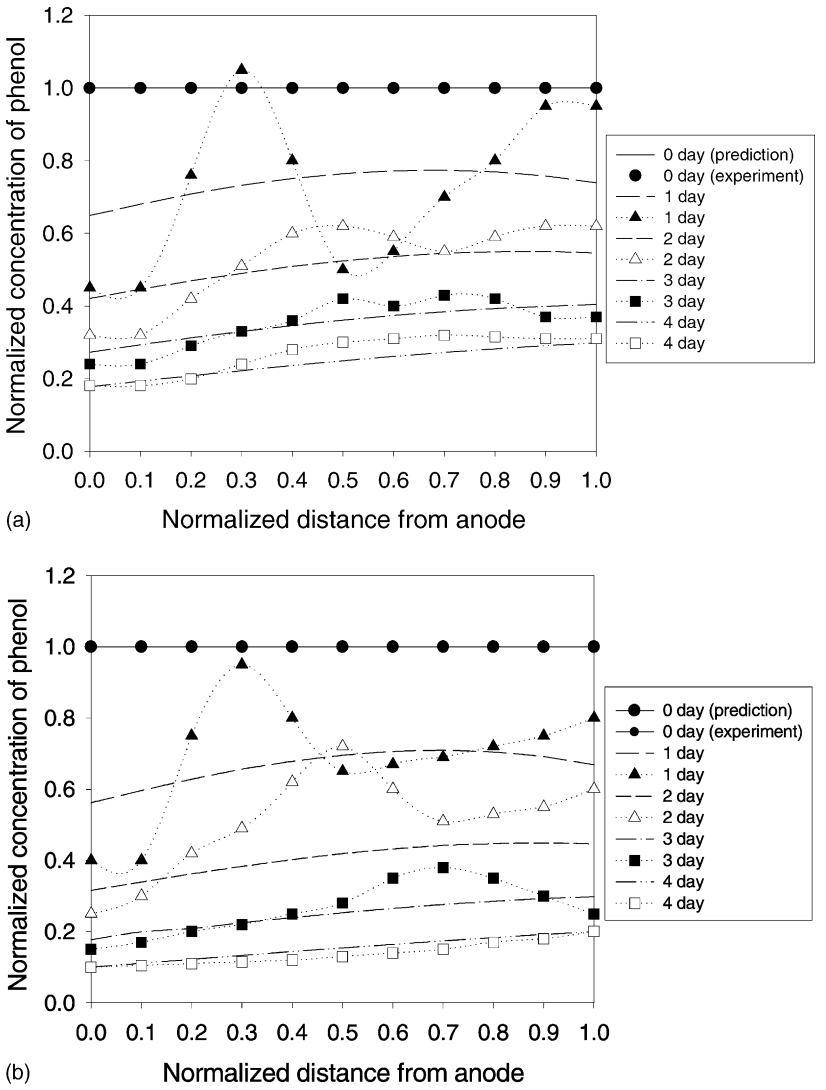

Fig. 5. Numerical analysis of the profiles of phenol existed in the pore water within the soil bed for Experiments I and II (spots: experimental data and lines: predicted data): (a) comparison between the experimental and predicted phenol profiles for Experiment I with chemical conditioning of 0.25 M H_2SO_4 in the cathode reservoir, (b) comparison between the experimental and predicted phenol profiles for Experiment II with chemical conditioning of 0.1 M NaOH and 0.25 M H_2SO_4 in the anode and the cathode reservoir, respectively.

chemical conditioning at the anode reservoir increased the electroosmotic flow toward the cathode and the removal of phenol from the soil, the increase in the alkaline concentration of the anode-purging solution did not significantly improve the removal rate of phenol. Table 3 summarizes the removal efficiency of phenol from the kaolinite soil in 4 days. The results shows the predicted operation time when 95% of phenol has been removed with the

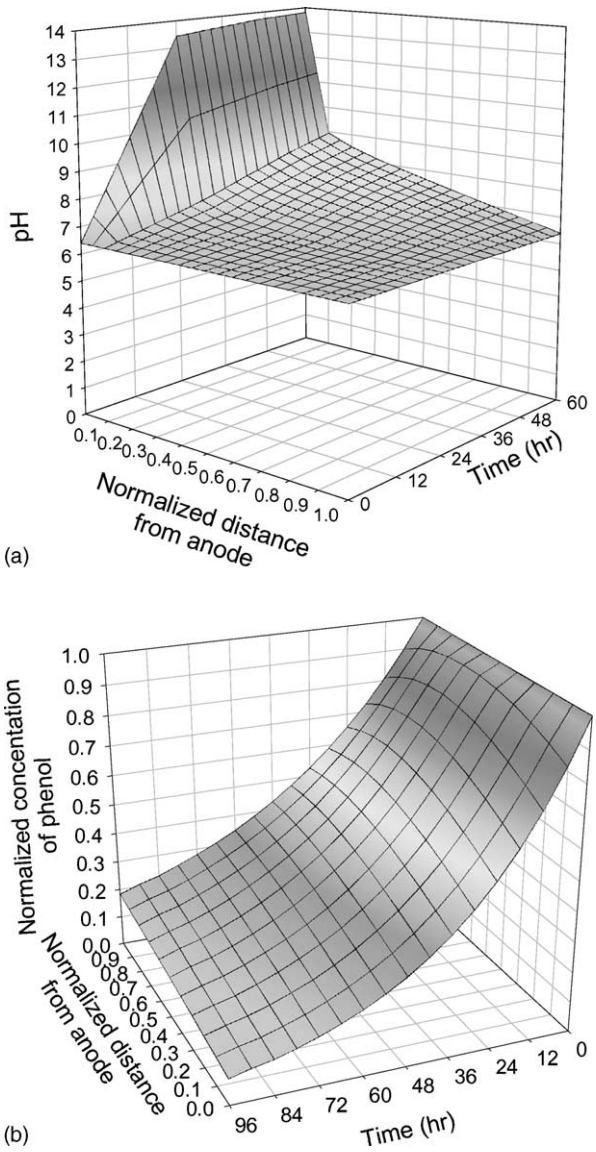

Fig. 6. Numerical analysis for an experiment with chemical conditioning of 4 M NaOH and 0.25 M H_2SO_4 in the anode and the cathode reservoir, respectively: (a) a 3D plot of the predicted pH profile of the pore water, (b) a 3D plot of the predicted profile of phenol existed in the pore water within the soil bed.

concentration of the NaOH solution used to neutralize the proton generated at the anode reservoir, implying that using chemical conditioning at the anode reservoir is more effective than increasing the alkaline concentration of the anode-purging solution for the removal of phenol from the soil. Moreover, the use of chemical conditioning at the anode reservoir

Table 3
Removal efficiency of phenol from the kaolinite soil in 4 days (I) and the required time to accomplish average 95% removal efficiency through the whole soil bed (II) with respect to the concentration of NaOH anode-purging solution

Concentration of NaOH anode-purging solution (M)	I (%)	II (h)
0	75	237
0.1	84.7	177.6
4	86.1	169.3

significantly can reduce the operation time to remove phenol from the soil bed, eventually resulting in lowering the operation cost by decreasing the energy consumption.

It was estimated that, to remove 95% of phenol from the soil, fresh anode-purging solution would be added after 102 h and then again at 155.7 h to prevent the anode-purging solution from being very acidic after 0.1 M NaOH anode-purging solution had been initially added. Using 4 M NaOH anode-purging solution initially, addition of a purging solution was not required throughout the operation.

4. Conclusions

The numerical method used in this study reasonably estimated the pH and phenol profiles in the soil bed. The proposed equations for predicting pH variations in both electrode reservoirs corresponded reasonably well with the experimental data. It was also determined that the given equations were useful to determine flux boundary conditions as well as injection time of the anode-purging solution. In the prediction of pH profiles in the soil bed, the time-averaging dispersion coefficient was used to include the averaging effect of the velocity profile on a one-dimensional transport and gave the better agreement between the experimental and predicted data. The numerical analysis revealed that using a basic solution for anode-purging expedite the phenol removal from the soil bed and reduced the operation time compared with the process without the chemical conditioning, while increasing the concentration of the alkaline anode-purging solution was not effective. Findings of the optimal chemical conditioning in this study may provide the guidelines to practice improved electrokinetic process in removing phenol from kaolinite soil.

Acknowledgements

This research was supported by the Korea Research Foundation (Project No. 1997-001-E00576).

References

[1] R.F. Probstein, P.C. Renaud, in: Proceedings of the Process of Workshop on Electrokinetic Treatment and its Application in Environmental Geotechnical Engineering for Hazardous Waste Site Remediation, University of Washington, Seattle, WA, 4–5 August 1986.

[2] A.P. Shapiro, Electroosmotic Purging of Contaminants from Saturated Soils, Ph.D. Thesis, Massachusetts Institute of Technology, Cambridge, MA, 1990.
[3] S.V. Ho, C.J. Athmer, M.A. Heitkamp, J.M. Brackin, Environ. Sci. Technol. 29 (1995) 2528.
[4] L.J. West, D.I. Stewart, A.M. Binley, B. Shaw, Eng. Geol. 53 (1999) 205.
[5] S.-O. Kim, S.-H. Moon, K.-W. Kim, Water, Air, Soil Pollut. 125 (2001) 259.
[6] S.-O. Kim, K.-W. Kim, J. Hazard. Mater. B85 (2001) 1995.
[7] M.M. Page, C.L. Page, J. Environ. Eng. 128 (2002) 208.
[8] A. Ugaz, S.P. Uppala, R.J. Gale, Y.B. Acar, Chem. Eng. Commun. 129 (1994) 183.
[9] B.E. Reed, M.T. Berg, J.C. Thompson, J.H. Hatfield, J. Environ. Eng. 121 (1995) 805.
[10] Y.B. Acar, R.J. Gale, G. Putnam, J.T. Hamed, in: Proceedings of the 2nd International Symposium on Environmental Geotechnology, Shanghi, China, 14–17 May 1989, Envo Publishing, Bethlehem, PA, 1989, pp. 25–38.
[11] Y.B. Acar, J. Hamed, R.J. Gale, G. Putnam, Acid/Base Distribution in Electroosmosis, Bulletin of the Transportation Research, Record No. 1288, Soils Geology and Foundations, Geotechnical Engineering, 1990, pp. 23–34.
[12] Y.B. Acar, H. Li, R.J. Gale, J. Geotech. Eng. 118 (1992) 1837.
[13] S.-O. Kim, S.-H. Moon, K.-W. Kim, Environ. Technol. 21 (2000) 417.
[14] S.K. Puppala, A.N. Alshawabkeh, Y.B. Acar, R.J. Gale, M. Bricka, J. Hazard. Mater. 55 (1997) 203.
[15] A.N. Alshawabkeh, Y.B. Acar, J. Environ. Sci. Health A27 (1992) 1835.
[16] A.N. Alshawabkeh, Y.B. Acar, J. Geotech. Eng. 122 (1996) 186.
[17] Y.B. Acar, L. Haider, J. Geotech. Eng. 116 (1990) 1031.
[18] C.D. Shackelford, D.E. Daniel, J. Geotech. Eng. 117 (1991) 467.
[19] M. Niinae, T. Aoe, W. Kishi, T. Sugano, J. Mining Mater. Process. Inst. Jpn. 114 (1998) 801.
[20] C.A.J. Fletcher, Computational Techniques for Fluid Dynamics, Springer-Verlag, Berlin, 1990, p. 216.
[21] R.M. Menon, Numerical modeling and experimental studies on electro-kinetic extraction, Ph.D. dissertation, Department of Civil Engineering, Texas A&M University, College Station, 1996.
[22] A.T. Yeung, S. Datla, Can. Geotech. J. 32 (1995) 569.
[23] P.B. Lorenz, Clays Clay Miner. 17 (1969) 223.
[24] B.E. Logan, Environmental Transport Processes, Wiley, New York, 1999, p. 358.
[25] D.R. Lide, H.P.R. Frederikse, CRC Handbook of Chemistry and Physics, CRC Press, Boca Raton, FL, 1994, p. 5.90.
[26] R.A. Jacobs, R.F. Probstein, AIChE J. 42 (1996) 1685.
[27] A.J. Bard, L.R. Faulkner, Electrochemical Methods, Wiley, New York, 1980, p. 67.